$ sciendo

Advances in Manufacturing Science and Technology

Diffusion Path in Ternary One-Phase Systems: An Overview

D. Serafin , W. J. Nowak, P. Wierzba, S. Wędrychowicz, B. Wierzba*

Rzeszow University of Technology, al. Powstańców Warszawy 12, 35-959 Rzeszów, Poland

Abstract

In this article, the fundamental questions concerning the diffusion path, in particular, what is the shape of diffusion path in ternary systems and how to approximate it from the initial concentration profile, will be answered. The new rules were found which allow for determining the diffusion path from a known initial concentration of the components. This approximation will allow for designing new materials without a time-consuming numerical simulation of the full system of equations. It is shown that the difference in intrinsic diffusion coefficients determines the up-hill diffusion.

Keywords

inter-diffusion • diffusion path • up-hill diffusion

1. Introduction

The literature devoted to the theory of partial differential equations is very extensive. It shows the methodology for solving very complex problems regarding the modeling of complex natural phenomena. These phenomena are described using nonlinear partial differential equations [1–9]. The literature also presents the enormity of progress made in the theory and application of nonlinear partial differential equations. The creators of this progress include Hormander [10, 11], Lax [12], Lions [13-15], Villani [16], and Tao [17]. The aforementioned manuscripts are concerned with the problems of the existence and uniqueness of solutions and the creation of new Banach and Sobolev spaces. The partial nonlinear differential equations, such as Navier–Stokes, Boltzmann, and Hamilton–Jacobi equations, were considered [18–22].

2. Methods

The most known method for calculating the diffusion phenomena in ternary couples is the Darken method [23]. In this method, the drift velocity was introduced. The drift velocity is a common velocity for each component and equals to the average of the diffusion fluxes:

$$v^{\text{drift}} = \sum_{i=A,B,C} D_i \frac{\partial N_i}{\partial x} \qquad (1)$$

The drift velocity is calculated from mass conservation laws for each component:

$$\frac{\partial N_i}{\partial t} + \frac{\partial}{\partial x}\left(N_i v_i^d + N_i v^{\text{drift}} \right) = 0, \qquad i = A, B, C \qquad (2)$$

Summation of the mass conservation and assumption, that is $N_A + N_B + N_C = 1$, allows for the determination of the drift.

In the literature, the diffusion path plays an important role in diffusion phenomena. The diffusion path is, by definition, a mapping of the stationary concentrations onto the isothermal section of the equilibrium phase diagram [24, 25]. The experimental determination of the diffusion (reaction) path during the diffusion couple experiments allows for the determination of many phenomena, such as the order of the product layers, their morphology, and their compositions [26]. The diffusion path connects initial compositions of the diffusion couple and can go across the single-, two-, and three-phase fields (in ternary systems). It starts at the composition of one alloy and ends at the other [24]. The possibility of mapping the concentration profiles onto the ternary isotherm has been postulated in 1 out of the 17 theorems by Kirkaldy and Brown [27] for the diffusion path.

The investigations presented in this article concern the determination of diffusion paths for physical systems. The solution to this problem consists of determining the classical solution of the system of nonlinear differential equations in the sense of the definition given by Evans [28].

Corresponding author: Bartek Wierzba

E-mail: bwierzba@prz.edu.pl

The proposed solution of the model in the present article is that the solution of the system of partial differential equations can be achieved by replacing it with linear and nonlinear algebra theorems. This solution allows fordetermining the diffusion path for any element system.

In this article, the additional observations describing the diffusion paths are shown. The ternary, one-phase diffusion path is analyzed. The family of functions will be presented (in the diffusion couples, the composition of one side is changed and the other side stays unchanged). It will be shown that there exists a composition that for different diffusion coefficients, the drift velocity is zero. Moreover, the theorem describing the up-hill diffusion will be presented.

3. Results

The Darken method was used for calculating the family of the diffusion couples in the ternary *A-B-C* system. The concentration was changed only on one side of the diffusion couple. The concentration of component *A* was constant, while the concentrations of *B* and *C* components were changed. The established components' concentrations in the members forming the diffusion couples are presented in Table 1.

The diffusion coefficients were constant for each component, $D_A = 10^{-10}$ and $D_B = D_C = 10^{-11} \text{ cm}^2\text{s}^{-1}$. The calculation time was 36,000 s and the temperature was set at 1273 K. The concentration profiles of component *A* were constant. The family functions of the concentration for *B* and *C* components are presented in Figure 1.

The up-hill diffusion is shown in *B* component's concentration profiles for samples 1–6. For the last two samples (7 and 8), the up-hill diffusion is not observed. However, the up-hill diffusion can be observed in *C* component's profile for these samples. Thus, this observation leads to the fact that the up-hill diffusion depends on the difference in values between the diffusion coefficients of the components and initial concentration of the samples. The corresponding drift velocity is presented in Figure 2.

Table 1. The established components' concentrations in the members of the diffusion couple

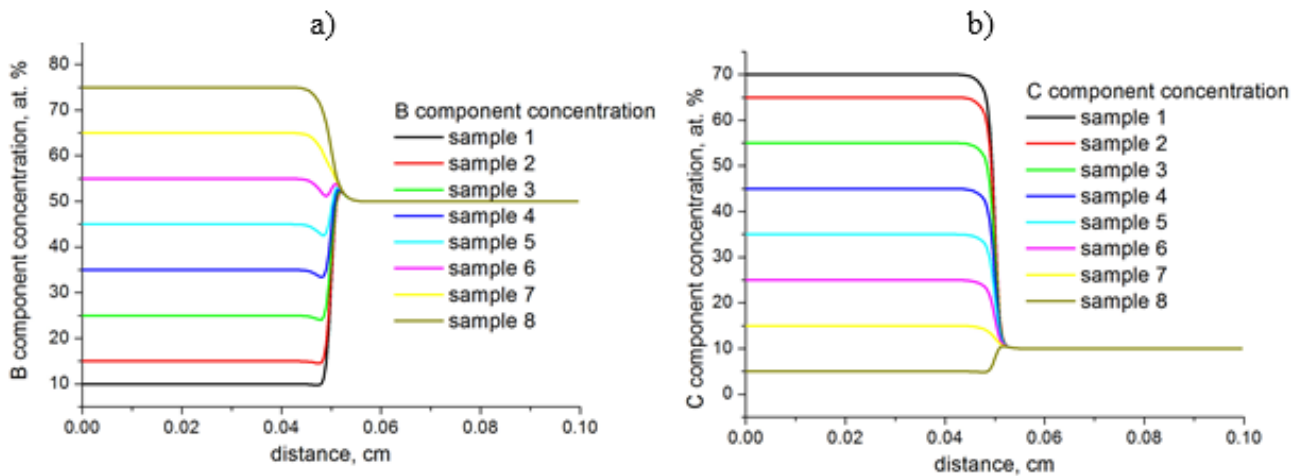| Sample no	Left member of the diffusion couple (at.%)			Right member of the diffusion couple (at.%)		
	A	B	C	A	B	C
1		10	70			
2		15	65			
3		25	55			
4	20	35	45	40	50	10
5		45	35			
6		55	25			
7		65	15			
8		75	5			

Figure 1. The family functions of concentration profiles of **(A)** *B* and **(B)** *C* components.
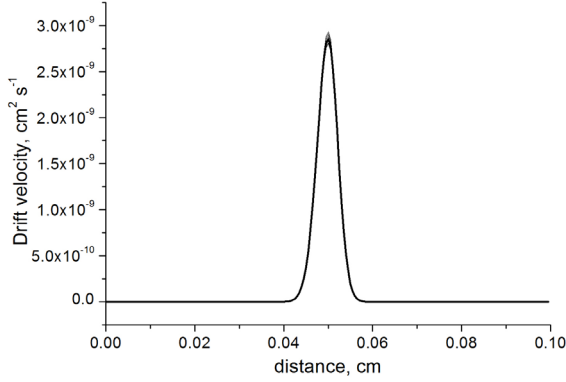
Figure 2. The family functions of drift velocity for different diffusion couples.

The following theorem concerning the up-hill diffusion [29] can be proved:

Theorem: *To generate the up-hill diffusion in the ternary system in the third component, the diffusion coefficient of the second component must be different from the diffusion coefficient of the first component; for example:*

$$D_2 > D_1 \tag{3}$$

Proof. Let us assume that we have mass transport in the ternary system – diffusion couple and diffusion coefficients of the components are composition-independent. To solve the problem of the generation of up-hill diffusion, we will choose the Darken method for ternary systems. The unknown molar ration can be determined from the mass conservation law with some initial and boundary functions:

$$\left.\begin{array}{l} \dfrac{\partial N_i}{\partial t} = \dfrac{\partial}{\partial x}\left(D_i \dfrac{\partial N_i}{\partial x} - N_i \sum_{j=1}^{3} D_j \dfrac{\partial N_j}{\partial x} \right), \\[2mm] N_i(0,x) = N_i^0, \\[2mm] \dfrac{\partial N_i}{\partial x}(t, \pm\Lambda) = 0. \end{array}\right\} i = 1,2,3 \tag{4}$$

where N_i^0 denotes the initial (for $t = 0$) molar ratio and Λ denotes the boundary of the system.
Moreover, the following relation holds:

$$N_1 + N_2 + N_3 \equiv 1 \tag{5}$$

Let us assume that for some distance $x_* \in [-\Lambda, \Lambda]$ and time t_*, the molar ratio of the third component is maximal; thus,

$$\frac{\partial N_3(t_*, x_*)}{\partial t} > 0 \tag{6}$$

and

$$\frac{\partial N_3(t_*, x_*)}{\partial x} = 0 \tag{7}$$

$$\frac{\partial^2 N_3(t_*, x_*)}{\partial x^2} \leq 0 \tag{8}$$

Thus, the mass conservation for the third component can be rewritten as follows:

$$\frac{\partial N_3}{\partial t} = (D_2 N_3 + D_3(1 - N_3)) \frac{\partial^2 N_3}{\partial x^2} - (D_1 - D_2) N_3 \frac{\partial^2 N_1}{\partial x^2} \tag{9}$$

The following inequality can be assumed:

$$(D_2 N_3 + D_3(1 - N_3)) \left| \frac{\partial^2 N_3}{\partial x^2} \right| < (D_2 - D_1) N_3 \frac{\partial^2 N_1}{\partial x^2} \tag{10}$$

because $\dfrac{\partial N_3}{\partial t} > 0$ and $(D_2 N_3 + D_3(1 - N_3)) \dfrac{\partial^2 N_3}{\partial x^2} \leq 0$ thus

$$(D_2 - D_1) N_3 \frac{\partial^2 N_1}{\partial x^2} > (D_2 N_3 + D_3(1 - N_3)) \left| \frac{\partial^2 N_3}{\partial x^2} \right| \tag{11}$$

Thus, the up-hill diffusion must be generated in the third component in time t_* at distance x_*:

$$\left. \frac{dN_3}{dt}(t, x_*) \right|_{t=t_*} > 0 \tag{12}$$

and finally exists ε so that

$$\frac{\partial N_3}{\partial t}(t, x_*) > 0, \quad N_3(t, x_*) > N_3(t_*, x_*), \quad \text{for every } t \in [t_*, t_* + \varepsilon]. \tag{13}$$

The diffusion paths of *A* and *B* and *A–C* family functions are presented in Figure 3.

The drift velocity is the same for each sample. The interesting observation can be made from Figure 3. In particular, the sign of the second derivative is changing during the process; only the initial compositions were different. The diffusion paths of *A–C* and *B* and *C* components are almost "linear" for sample 7 (Figure 4).
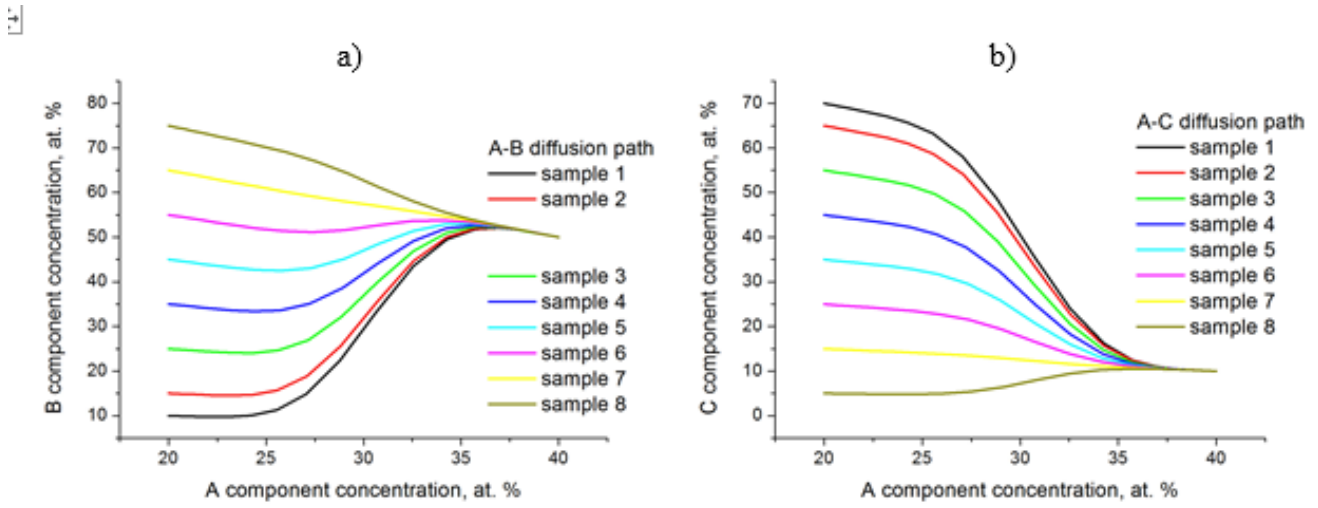
Figure 3. The family functions of diffusion path of **(A)** *A* and *B* and **(B)** *A–C* components.
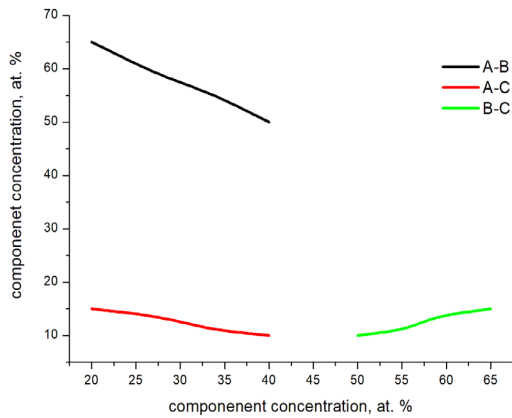

Figure 4. The diffusion paths for sample 7.

This feature is described by the Kirkaldy theorem: when the diffusion coefficients are constant and of the same value in the system, the diffusion path is linear. However, in our analysis, the *A* and *B* components' diffusion coefficients are different. Thus, such a composition exists in the diffusion couple indicating that the diffusion paths will be the same (linear) like in the situation when the drift velocity is constant. These concentrations can be determined by optimization techniques – equating the drift velocity to zero:

$$v^{\text{drift}} = \sum_{i=A,B,C} D_i \frac{\partial N_i}{\partial x} = 0 \tag{14}$$

Assuming that the sum of molar ratios of components is equal to 1, $N_A + N_B + N_C = 1$ and eliminating *C* component in Eq. (14) are as follows:

$$D_A \frac{\partial N_A}{\partial x} + D_B \frac{\partial N_B}{\partial x} + D_C \frac{\partial (1 - N_A - N_B)}{\partial x} = 0 \tag{15}$$

thus

$$(D_A - D_C)\frac{\partial N_A}{\partial x} + (D_B - D_C)\frac{\partial N_B}{\partial x} = 0 \tag{16}$$

grouping the elements gives:

$$\frac{\partial N_A}{\partial x} \Big/ \frac{\partial N_B}{\partial x} = -\frac{(D_B - D_C)}{(D_A - D_C)} \tag{17}$$

and finally, the following relation is assumed, when the diffusion path is a straight line (when diffusion coefficients are constant):

$$\frac{\partial N_A}{\partial N_B} = -\frac{(D_B - D_C)}{(D_A - D_C)} \tag{18}$$

The second family of the functions was the diffusion couples where the concentrations of *A* and *C* components were changed at one side of the couple (Table 2).
The concentration profiles of *A* and *C* components are presented in Figure 5. The up-hill diffusion can be observed for samples 4–8. However, for samples 1–4, the up-hill is observed in *B* component (Figure 6).
In this case, the drift velocity is not constant. Moreover, the sign is changed; for samples 1–4, the drift velocity is positive, while for samples 5–8, the drift velocity is negative (Figure 7).

Table 2. The established component's concentrations in the members of diffusion couple

Sample no	Left member of the diffusion couple (at.%)			Right member of the diffusion couple (at.%)		
	A	B	C	A	B	C
1	20		70			
2	25		65			
3	30		60			
4	35		55			
5	40	10	50	40	50	10
6	45		45			
7	50		40			
8	55		35			
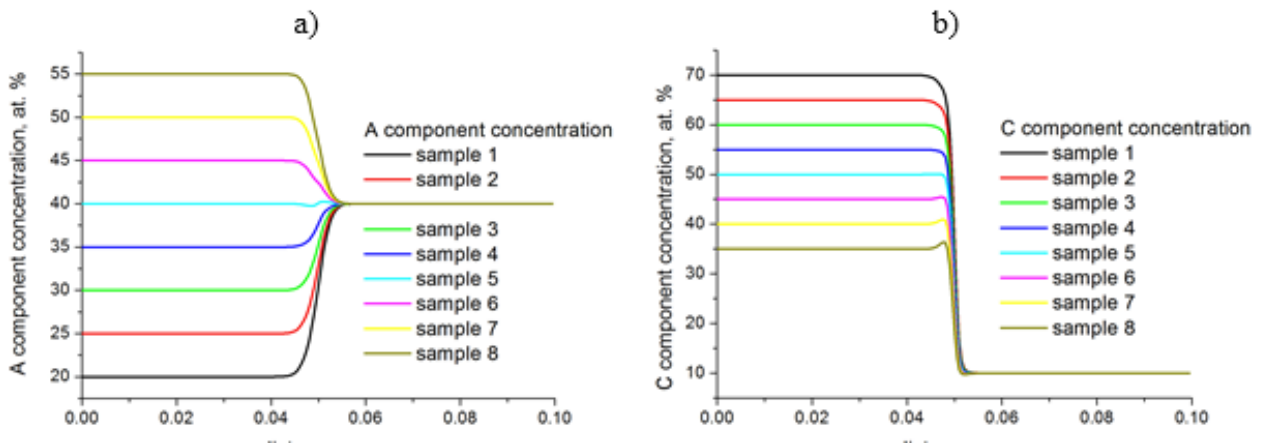
Figure 5. The family functions of concentration profiles of **(A)** *A* and **(B)** *C* components.
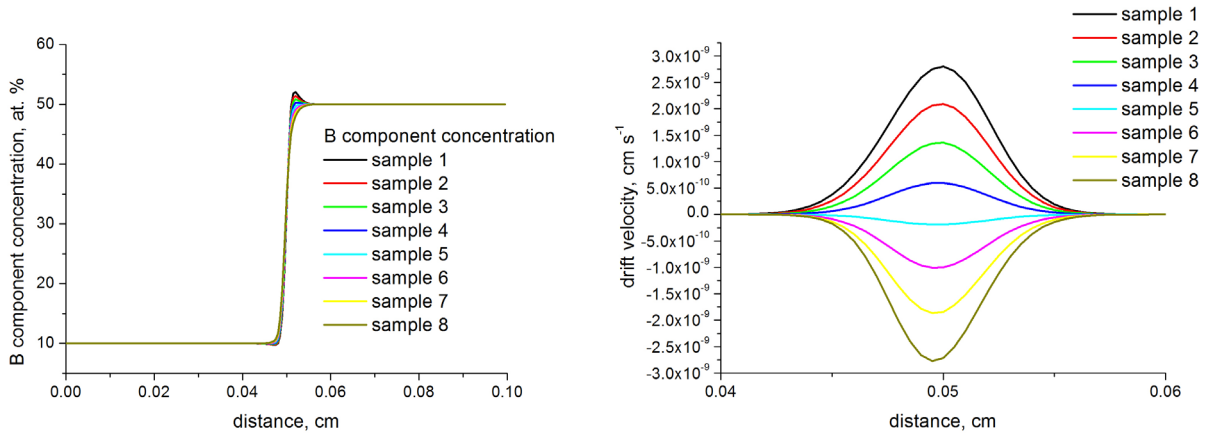

Figure 6. The family functions of concentration profiles of component *B*. **Figure 7.** The family functions describing the drift velocity.
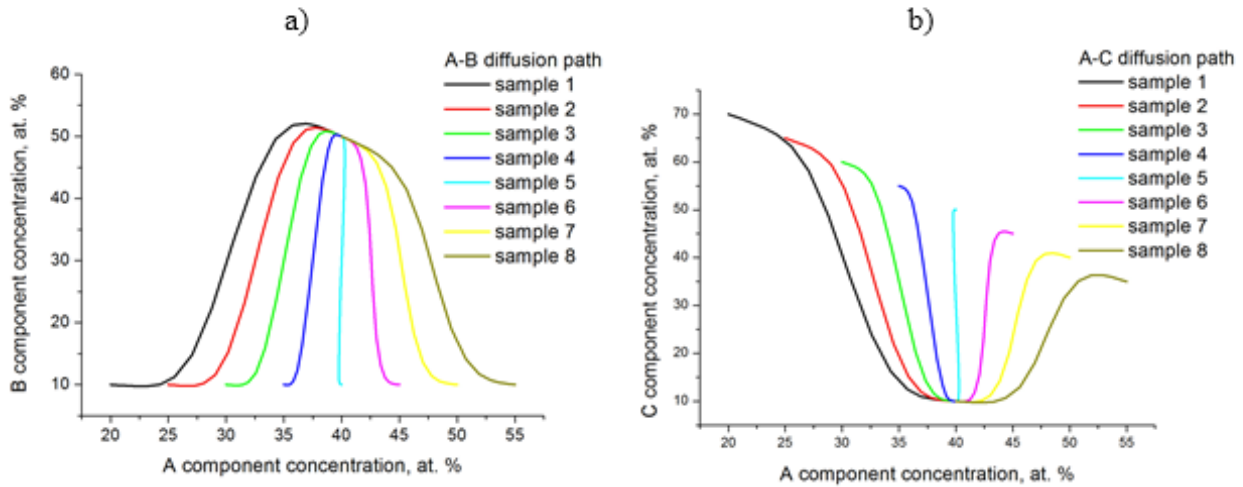
Figure 8. The family functions of diffusion path of **(A)** *A* and *B* and **(B)** *A*–*C* components.

Thus, there exists the concentration of *A* and *C* components for which the drift velocity is zero. It can be seen that the drift velocity influences the size of the up-hill diffusion can be observed at the concentration profile. The diffusion paths of *A* and *B* and *A*–*C* components are shown in Figure 8.

The next results are approximated for a different set of diffusion coefficients (Table 3). The calculation time was 36,000 s and the temperature was set at 1273 K. The concentrations of the end members of diffusion couple used for this calculation are presented in Table 2 for sample 1.

The concentration profiles for samples 1–5 are presented in Figure 9.

The qualitative difference can be observed. For example, for samples 1–4, the up-hill diffusion is presented in component *B*. For sample 5, the up-hill is presented in component *B*. Moreover, for samples 1–4, the concentration profiles are very similar; however, the drift velocity differs (Figure 10).

The drift velocity increases with the increase of diffusion coefficients. Thus, the highest (at Matano position) is for sample 5. All of the three diffusion coefficients influence the drift velocity. The diffusion paths for samples 1–5 are presented in Figure 11. It can be observed that for samples 1 and 3,

the diffusion paths are similar. Thus, the proportion of the diffusion coefficients is an important factor. The proportions of diffusion coefficients of samples 1 and 3 are the same. The diffusion paths of samples 3 and 5 are not similar to each other. In sample 3, the ratio of diffusion coefficients of *A* and *B* components is equal to 10.

4. Conclusions

After our analysis, the following conclusions can be described: When $D_A > D_B$, the up-hill diffusion phenomena can be found either in component *B* or *C*. When $D_A = D_B$, the up-hill can be found in component *A*.

The up-hill diffusion does not appear in the component of the highest composition difference.

The up-hill diffusion determines the direction of the diffusion path – see sample 5 in Figure 10 (the up-hill diffusion is found in component *A*).

The drift velocity depends mainly on the diffusion coefficients. The initial concentration has a small impact on it.

Table 3. The data used for simulations of diffusion phenomena

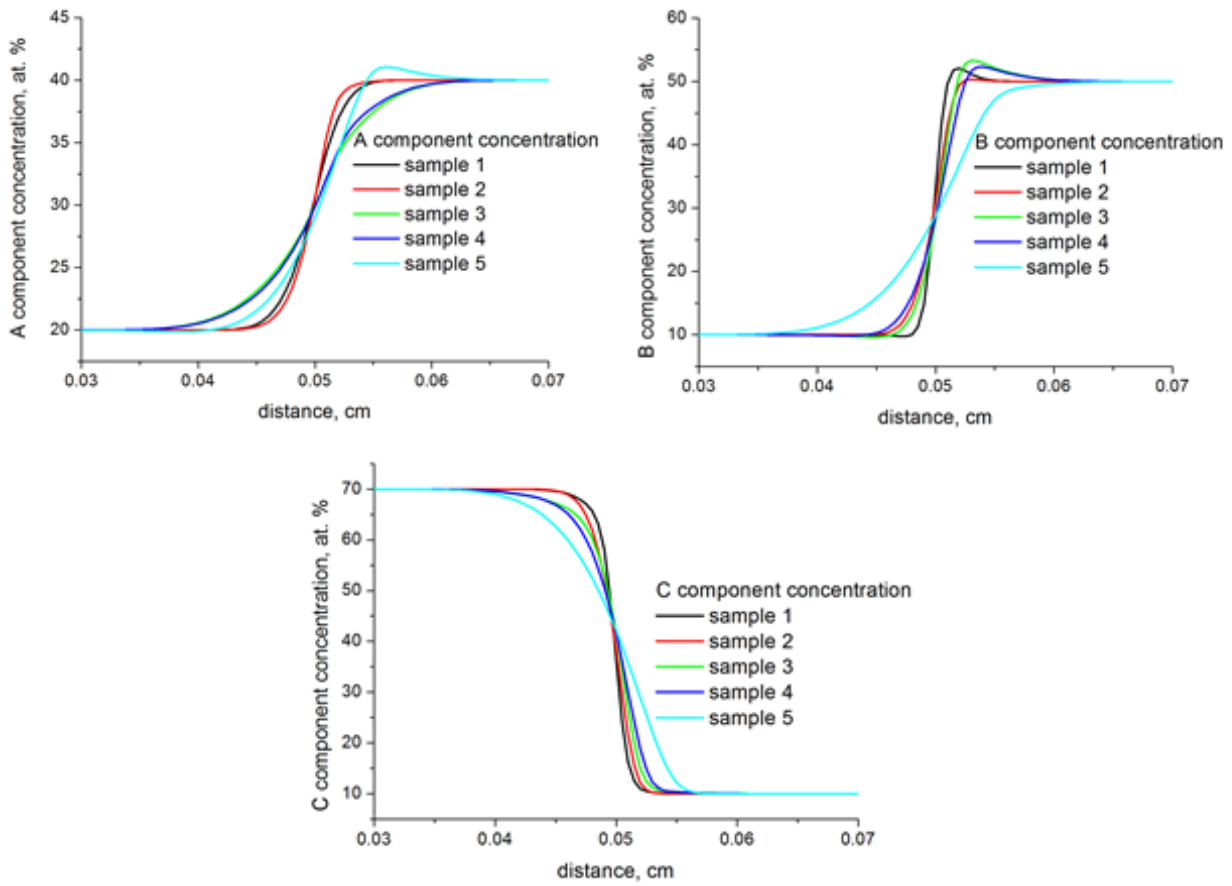| Sample no.	D_A (cm²s⁻¹)	D_B (cm²s⁻¹)	D_C (cm²s⁻¹)
1	10^{-10}	10^{-11}	
2	10^{-10}	5×10^{-11}	
3	5×10^{-10}	5×10^{-11}	10^{-11}
4	5×10^{-10}	10^{-10}	
5	5×10^{-10}	5×10^{-10}	

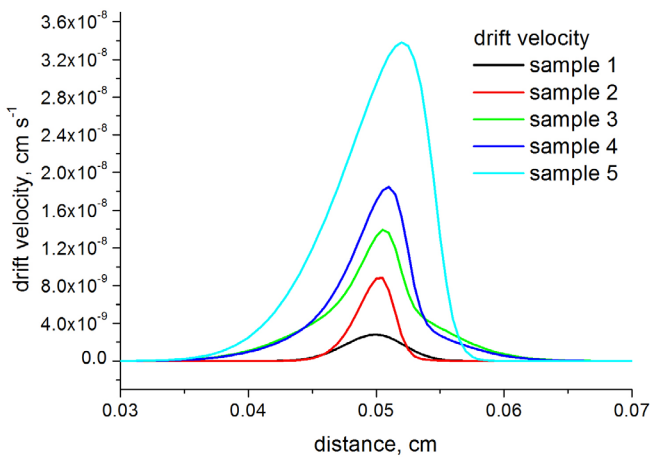**Figure 9.** The concentration profiles for samples 1–5.

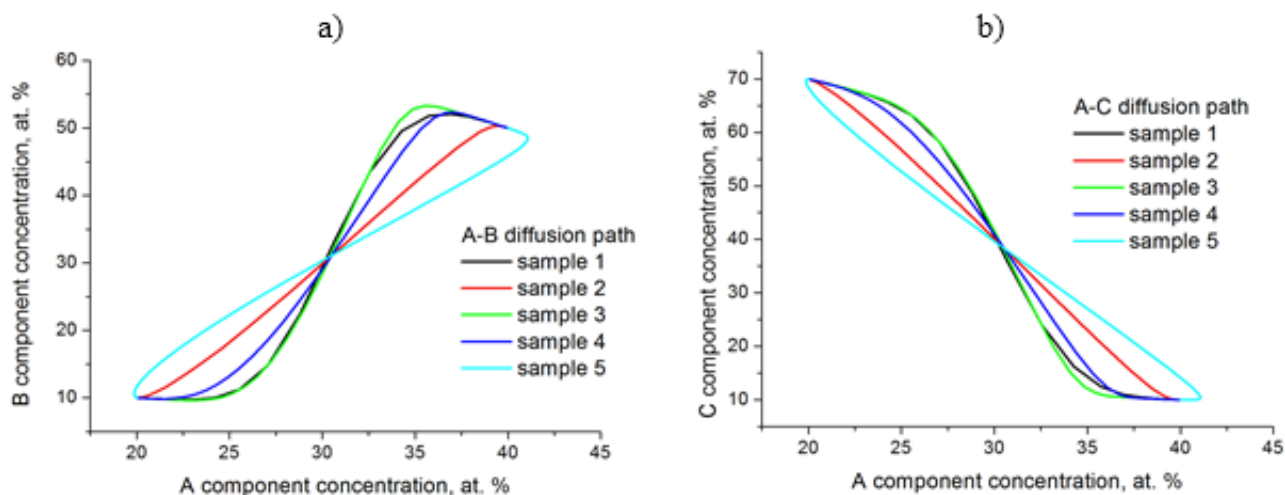**Figure 10.** The drift velocity of samples 1–5.

Figure 11. The family functions of diffusion path of **(A)** *A* and *B* and **(B)** *A–C* components.

References

[1] R.A. ADAMS: Sobolev spaces. Academic Press, New York 1975.

[2] V. Arnold: Mathematical methods of classic mechanics. Springer, New York 1986.

[3] V. ARNOLD and B.A. KHESIN: Topological methods in hydrodynamics. Springer, New York 1998.

[4] V. BARBU: Nonlinear semi groups and differential equations in Banach spaces. Springer Netherlands, Noordhoff, 1976.

[5] M.S. BERGER: Nonlinearity and functional analysis. Academic Press, New York 1977.

[6] A. BENSOUSSAN, J.L. LIONS, G. PAPANIKOLAOU: Asymptotoc analysis for periodic structures. Elsevier, North Holland 1978.

[7] H. BREZIS: Functional analysis, Sobolev spaces and partial differential equations. Springer, New York 2011.

[8] F.E. BROWDER: Nonlinear operators and nonlinear equation in Banach spaces. American Mathematical Society 1976.

[9] C. CERCIGNANI: The Boltzmann equations and its applications. Springer, New York 1988.

[10] L. HORMANDER: The analysis of linear partial differential operators, vol. 1-4. Springer, Berlin 1983.

[11] L. HORMANDER: Fourier integral operators. I. *Acta Math*., **127**(1971), 79-189.

[12] P.D. LAX: Functional analysis. Wiley - Interscience, New York 2002.

[13] P.L. LIONS: Mathematical topics in fluid mechanics, Vol 1. Incompressible models, Clarendon Press, Oxford 2006.

[14] P.L. LIONS: Mathematical topics in fluid mechanics, Vol 2. Compressible models, Clarendon Press, Oxford 2006.

[15] P.L. LIONS: Generalization solutions of Hamilton Jacobi equations, Longman Harlow, Essex 1982.

[16] C. VILLANI: Topic in optimal transportation. American Mathematical Society 2003.

[17] T. TAO: An epsilon of room I: real analysis. American Mathematical Society 2010.

[18] C. FOIAS, et al.: Navier-Stokes equation and turbulence. Cambridge University Press, Cambridge 2001.

[19] V. GIRAULT, P.A. RAVIART: Finite element method for Navier-Stokes equations. Springer, Berlin 1986.

[20] R. TEMAM: Navier-Stokes equations. Theory and numerical analysis. Elsevier, North-Holland 1985.

[21] G. TOSCANI, C. VILLANI: Probability metrics and uniqueness of the solution to the Boltzmann equation for a Maxwell Gas. *J. Stat. Phys*., **94**(1999), 619-637.

[22] D. ZWILLINGER: Handbook of differential equations. Academic Press, New York 1984.

[23] L.S. DARKEN: *Trans. AIME*, **174**(1948), 184.

[24] M. DANIELEWSKI, B. WIERZBA, K. TKACZ-SMIECH: *Diffus. Found*., **1**(2014), 31.

[25] B. WIERZBA: *Physica A*, **454**(2016), 110-116.

[26] A.A. KODENTSOV, et al.: *J Alloys Compd*., **320**(2001), 207.

[27] J.S. KIRKALDY, L.S. BROWN: *Can. Metal. Q*., **2**(1963), 89.

[28] L.C. EVANS: Convergence methods for nonlinear partial differential equations. American Mathematical Society, 1990.

[29] K. HOLLY, M. DANIELEWSKI: *Phys. Rev. B: Condens. Matter Mater. Phys*., **50**(1994), 13336.